Preliminary Optical Performance of the SPRITE CubeSat Instrument

Maitland Bowen[a], Brian Fleming[a], Briana Indahl[a], Dmitry Vorobiev[a], Daniel Szewczyk[a], Kevin France[a], Luis V. Rodríguez-de Marcos[b], Manuel A. Quijada[c], and John J. Hennessy[d]

[a]Laboratory for Atmospheric and Space Physics, University of Colorado, Boulder CO 80303
[b]Catholic University of America and NASA Goddard Space Flight Center (CRESST II agreement), Greenbelt, MD 20771
[c]NASA Goddard Space Flight Center, Greenbelt MD 20771
[d]Jet Propulsion Laboratory, California Institute of Technology, Pasadena CA 91109

ABSTRACT

The Supernova remnants & Proxies for Reionization Testbed Experiment (SPRITE), a 12U CubeSat, will investigate tracers of galactic and cosmic structure in the far-ultraviolet (FUV) over a nominal two-year mission. These tracers include the escape of ionizing radiation from, as well as the mass and energy flows within, galaxies. To observe these processes, the SPRITE instrument employs a variety of advanced optics technologies that necessitate an extensive testing campaign prior to delivery. SPRITE's broadband mirror coatings, comprised of enhanced lithium fluoride over an aluminum deposition (eLiF) and overcoated with protective magnesium fluoride (MgF_2), operate with >70% reflectance to $\lambda > 1020$ Å. SPRITE is the orbital testbed for these new coatings, representing a significant improvement over the Hubble Space Telescope (HST) and the Far Ultraviolet Spectroscopic Explorer (FUSE), and qualifying these coatings for potential use on the Habitable Worlds Observatory (HWO). We demonstrate that this combination of coatings provides high throughput with low environmental degradation. We also present the results of component-level testing and instrument characterization of the SPRITE instrument.

Keywords: astronomy, astrophysics, satellites, optical design, ultraviolet spectroscopy

1. INTRODUCTION

The ultraviolet is the most sensitive spectral window to thermal emission from clusters of hot stars ($T_{eff} \sim 10^4 - 10^5$ K). Atomic and molecular transitions that trace the kinematic processes driving galactic evolution are observed in the far-UV (FUV; 912 - 2000 Å). In particular, observations in the 912 - 1200 Å bandpass, commonly referred to as the Lyman UV, quantify how massive stars impact their host galaxies and control the escape of ionizing radiation into the intergalactic medium (IGM). This makes the Lyman UV an extremely valuable source of information for galaxy evolution and cosmic structure formation. However, spectral imaging from an orbital platform in the Lyman UV has never been achieved with arcsecond-level angular resolution.[1]

The Supernova remnants & Proxies for Reionization Testbed Experiment (SPRITE) will fill this large and scientifically rich gap as the first dedicated FUV astrophysics mission launched into orbit in over a decade. Based at the Laboratory for Atmospheric and Space Physics (LASP) at the University of Colorado Boulder as part of the Colorado Ultraviolet Spectroscopy Program (CUSP), SPRITE is a 12U CubeSat mission that addresses how galaxies provide ionizing radiation to the intergalactic medium and how ionization and kinematic processes drive galactic evolution. The innovative optical design utilized on SPRITE also allows it to serve as a demonstration testbed for a future large (> 6m) ultraviolet/optical/infrared surveyor such as the Habitable Worlds Observatory (HWO). Both the technologies required for this future survey and the survey itself have been identified as priorities in the recommendations of *Pathways to Discovery in Astronomy and Astrophysics for the 2020s Decadal Survey*.[2] Figure 1 shows the SPRITE spacecraft in its flight configuration with its solar

Further author information: (Send correspondence to M.B.)
M.B.: E-mail: maitland.bowen@lasp.colorado.edu

panels and UHF antenna deployed. SPRITE is planned to launch into low-Earth orbit (LEO) in late 2024, with launch manifest pending.[3]

This proceeding describes the SPRITE instrument and its preliminary optical integration and testing campaign. Section 2 explains SPRITE's motivating science; Section 3 describes the instrument, its components, and optical testing; Section 4 briefly outlines future integration and testing.

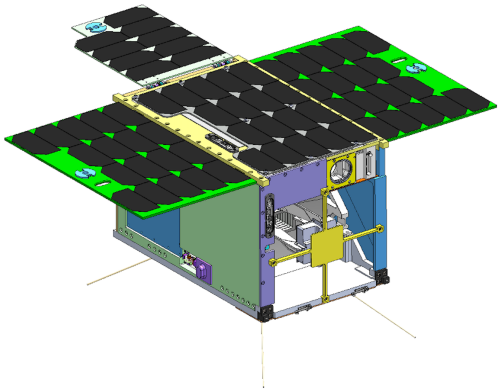

Figure 1: The SPRITE CubeSat CAD with solar panels and UHF antenna deployed. SPRITE is the first 12U-sized NASA SMD-funded astrophysics CubeSat.

2. SCIENCE OVERVIEW

SPRITE is designed to carry out three scientific surveys (see Indahl et al., in this Proceedings).[3] The first measures escaping ionizing radiation from a sample of low-redshift ($0.16 < z < 0.4$) star-forming galaxies, for which high sensitivity via high signal throughput and low backgrounds is essential. The second survey maps supernova remnants and star formation in the Milky Way and the Large and Small Magellanic Clouds (LMC and SMC, respectively) in the UV. The third measures the global structure of feedback in a small sample of local galaxies by "push-broom" mapping the FUV continuum and emission features, creating the first sub-arcminute three-dimensional spectral data cubes in this bandpass.

2.1 Lyman continuum escape survey

The mass and energy flows within galaxies are dictated by ionization and kinematic drivers that largely originate from hot, massive OB stars. These kinematic processes, including intense radiation, fast stellar winds, and metal dissipation in supernovae, are well-traced in the neutral and ionized atomic lines probed in the FUV.

The transition from neutral to ionized intergalactic medium (IGM) is one of the key signifiers of cosmic structure formation. The question of how much ionizing radiation escapes into the IGM from galaxies is critical to our understanding of the history of cosmic structure formation, especially the Epoch of Reionization (EoR). SPRITE's Lyman continuum (LyC) survey seeks to measure the LyC escape fraction, f_{esc}, or the fraction of ionizing radiation that escapes a galaxy relative to the radiation produced by the stars in that galaxy. These signals have expected fluxes of $F(\lambda) < 2 \times 10^{-16}$ erg cm^{-2} s^{-1} Å^{-1} for a low-redshift galaxy.[1]

At the epoch of reionization (z $\sim$ 6-10), f_{esc} cannot be measured directly, as the neutral fraction of the IGM is too high beyond a redshift of $z \sim 3$. Even the James Webb Space Telescope (JWST), for which observing the galaxies that drove reionization is a core scientific objective, cannot observe ionizing radiation directly at the EoR. Instead, redshifted UV and optical emission lines are used as proxies, which must be calibrated via direct measurements of escaping ionizing radiation from a selection of low-redshift galaxies. Therefore, constraining f_{esc} at low redshift is vital to cleanly interpret future observations of redshifted UV and optical emission lines. SPRITE will accomplish this by directly measuring f_{esc} in $\sim$ 50 nearby galaxies and active galactic nuclei (AGN) to the 2-5% level.

2.2 Spectral and spatial mapping surveys

The SPRITE mission will map the structures of a sample of targets in the FUV at sub-arcminute angular resolution and high spatial resolution using push-broom spectral mapping with a $1800'' \times 10''$ slit. These targets include nearby galaxies and supernova remnants, as well as regions of star formation in the Milky Way, LMC, and SMC. Figure 2 illustrates how the push-broom procedure will obtain spectra at each slit segment across the entire target to create a spectral and spatial map, using the Antennae Galaxies (NGC 4038/NGC 403) as an example target.

The resulting 3D (x,y,λ) data cube will provide the most comprehensive UV data set for some of the most well-studied objects in the local universe.[1] This data will include observations of dust attenuation, emission lines,

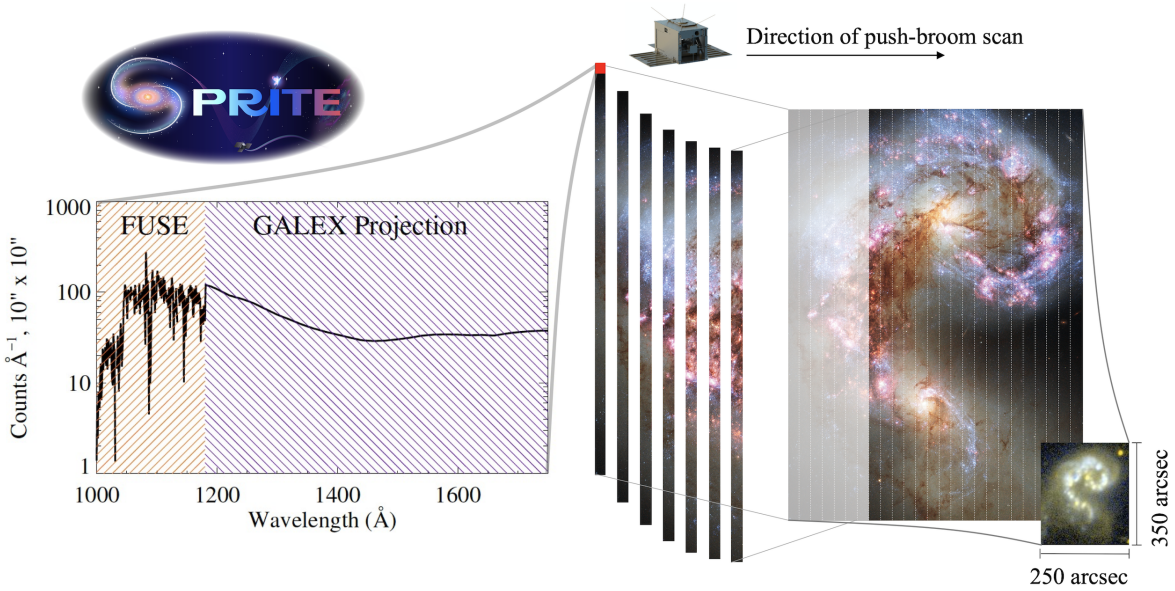

Figure 2: Illustration of the push-broom observation using the spectrum of NGC 4038/NGC 4039 obtained by the Far Ultraviolet Spectroscopic Explorer (FUSE) and extrapolated with simulated Galaxy Evolution Explorer (GALEX) data.

and ionized gas outflow features for some of the best known local galaxies. This will yield an unprecedented data set in the ultraviolet, where there has never been a sub-arcminute imaging spectrograph with this wavelength coverage and high spatial resolution.

3. INSTRUMENT OVERVIEW

SPRITE is the first NASA-funded 12U dedicated astrophysics CubeSat and the first orbital astrophysics instrument sensitive to the far-ultraviolet (FUV, 1000-1750 Å) since the Cosmic Origin Spectrograph (COS) deployed on HST. SPRITE's science instrument is comprised of a Cassegrain F/2.7 telescope, a diffraction grating, a cylindrical fold mirror, a microchannel plate (MCP) detector and its housing, and the SPRITE Calibration Channel (SCC), which will help track the stability of the mirror coatings and detector on-orbit. CAD models of the instrument are shown in Figure 3.

The idealized SPRITE raytrace design (Figure 4) has ~ 1.3 Å resolution for a resolving power of $\lambda/\Delta\lambda \approx 770 - 1350$ for its range of $1000 - 1750$ Å as well as a cross-dispersion resolution of 8-20″, depending on the location along the cross-dispersion axis of the instrument (i.e., the slit's long dimension). This makes SPRITE the first instrument with sub-arcminute imaging spectroscopic capability at $\lambda < 115$ nm. SPRITE also serves as a flight testbed and technology demonstration of the performance of the advanced mirror coatings and MCP detectors that will be utilized on a future large infrared/optical/ultraviolet space surveyor such as HWO.

The telescope, provided by Nu-Tek Precision Optical Corporation, is a Cassegrain design with an 18 cm x 16 cm primary mirror. Figure 4 shows the ray trace within the instrument. Light entering the aperture is reflected off the primary mirror to the secondary, where it is then reflected through a channel in the center of the primary mirror and focused onto the slit. The light then passes through the slit and its baffle to the concave abberation-correcting holographic grating provided by Horiba Jobin-Yvon, the same vendor that developed the HST-COS gratings. Holographic gratings were selected for SPRITE because they have better scattered light properties than mechanically ruled gratings, while a blazed grating was selected for high efficiency.[4] The diffracted light from the grating then reflects off a cylindrical tertiary mirror (M3) and is recorded on the MCP detector, which is described further in 3.2.

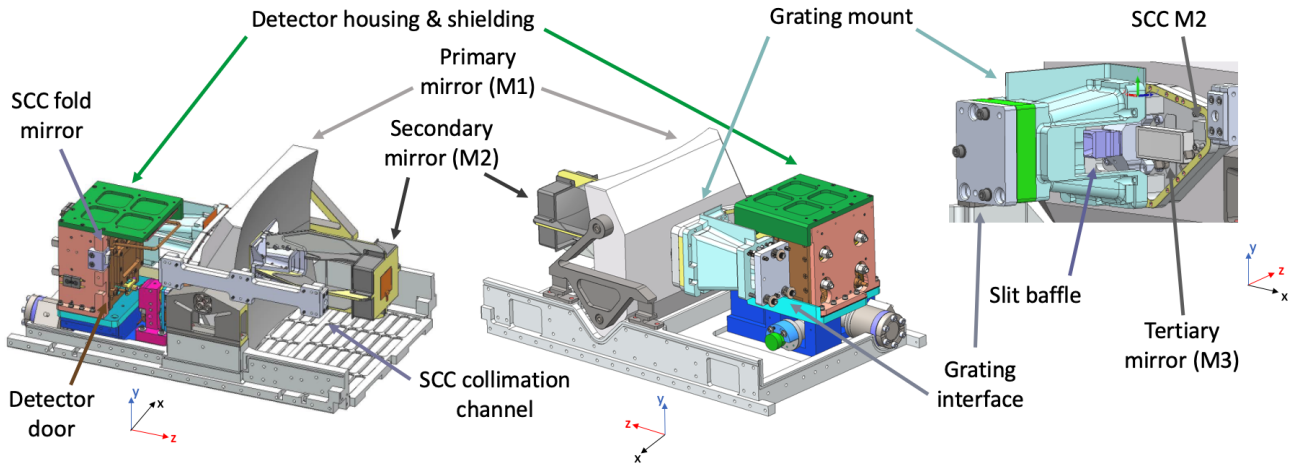

Figure 3: Left: Front view of the SPRITE instrument, composed of the telescope, spectrograph, and SCC. Center: Rear view of the instrument. The detector housing is secured to the baseplate via an intermediary mount to accommodate the detector's vacuum connection. Right: Interior view of the spectrograph. The slit baffle, grating mount, M3, and SCC M2 are all installed on an intermediary mount on the back of M1.

The SPRITE Calibration Channel (SCC) consists of a CaF_2 windowed mechanical collimation tube feeding a two-optic focuser. A flat mirror (SCC M1) directs the collimated beam to an off-axis parabolic focuser (SCC M2) to provide a co-aligned ∼3° FOV low-resolution imager. This imager is co-aligned with the spectrograph to provide a separate 1350 - 2000 Å image of bright targets for cross-calibration purposes, but using MgF_2 protected aluminum optics, the same coatings used on HST and several other prior missions. This calibration channel allows on-orbit degradation of the detector or the mirror coatings (described below in 3.1) to be disentangled, providing an independent assessment of the performance and stability of each new technology.

3.1 Optical Coatings

The most critical aspect for the throughput and bandpass of FUV instrumentation is the reflectivity of the mirror coatings. SPRITE utilizes advanced environmentally-resistant mirror coatings[5] which demonstrably exceed 80% reflectivity at 1100 Å. This is approximately 20% more than the conventional LiF+Al used on the Far Ultraviolet Spectroscopic Explorer (FUSE) and > 5 times more than the MgF_2 used on HST for observations at these wavelengths.[6] The coating process was refined over a ∼2-year timescale, with the heating method and fixtures developed and tested on mass models and witness samples.

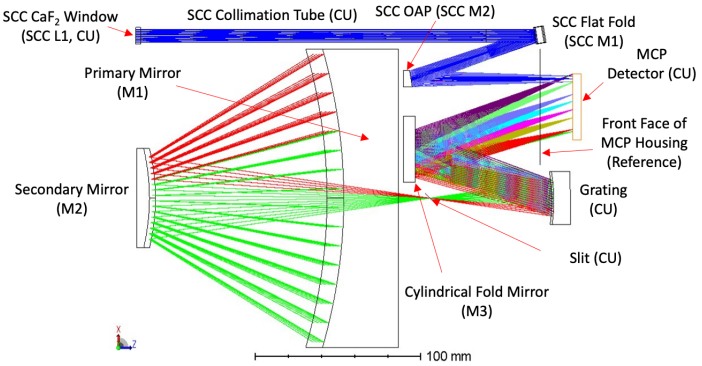

Figure 4: A ray trace showing light being focused by the telescope to the slit, where it travels through to the grating, the tertiary mirror, and then the detector. The light traveling through the collimation channel (SCC) to the detector is also shown.

Protected enhanced lithium flouride (eLIF) coatings were baselined in the LUVOIR surveyor concept study report, for which SPRITE is an essential orbital testbed.[7] While conventional LiF+Al coatings are deposited at room temperature, eLiF coatings are then post-annealed at elevated temperatures ($\sim 260°C$).[5] After deposition of the eLiF, the SPRITE optics are then shipped in hermetically sealed, N_2-filled shipping containers to NASA JPL where an ultrathin $\sim$ 20 Å capping layer of MgF_2 is applied via atomic layer deposition (ALD).[8]

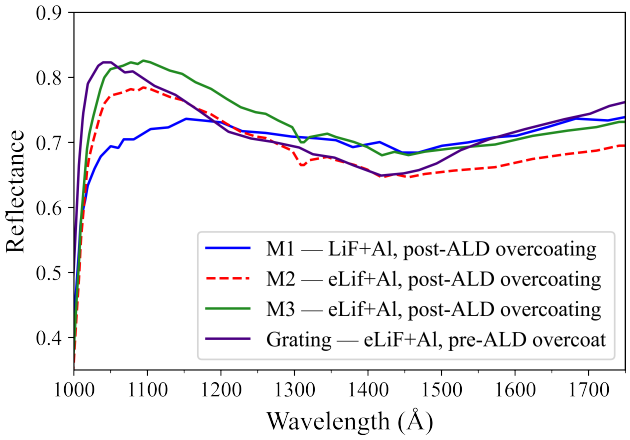

Figure 5: The measured reflectances of witness samples coated alongside each optic. Note that the grating witness was measured immediately after eLiF deposition, prior to MgF_2 overcoating.

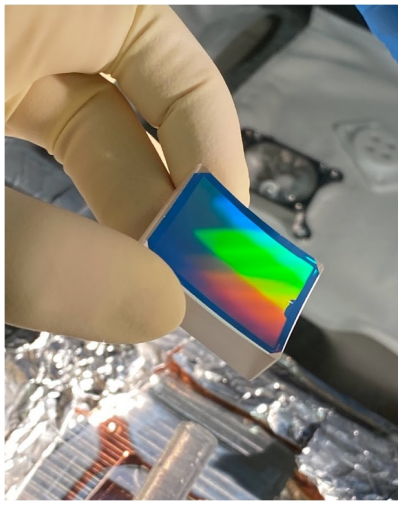

Figure 6: The flight grating after eLiF deposition at NASA GSFC.

Figure 5 shows the reflectances of the witness samples that were placed next to each SPRITE optic during the coating process. M1 and its witness sample were coated in conventional LiF+Al and protected with a MgF_2 capping layer; the witness sample demonstrated a peak reflectance of $\sim$ 73% at 1152Å. M3 and its witness sample were coated in eLiF followed by MgF_2, and the witness sample reflectance peaked at $\sim$ 82% at 1092Å. The grating shown in Figure 6 and its witness sample were coated in eLiF, and the witness sample reflectance was measured prior to MgF_2 overcoating with a peak reflectivity of $\sim$82% at 1043Å. Two witness samples were coated alongside M2, placed next to two adjacent sides of the optic, meaning that the projected reflectance of M2 relies more heavily on estimation than the other optics; based on the measurements of those witness samples. As such, the M2 reflectance in Figure 5 is an estimate based on both the peak reflectances of the witness samples and the shape of the M3 reflectance curve, as it is reasonable to expect that the coatings on M2 perform similarly to those on M3.

Conventional LiF+Al coatings, such as those used on FUSE, are hygroscopic, losing as much as 30% reflectivity as they degrade with exposure to humidity above 50%.[9] When compounded through the reflections across four optics, this loss would severely impair the instrument throughput. The MgF_2 capping layer is essential for SPRITE as it provides protection for the hygroscopic LiF from water vapor. Because the MgF_2 layer is ultrathin, it does not significantly reduce the reflectivity of the underlying Al+LiF coating. A witness sample coated in eLiF without MgF_2 that was exposed to up to 30% relative humidity (RH) for five months showed a 16% decrease in reflectance at $\lambda = 103$ nm; witness samples that were overcoated with MgF_2 exposed to 30% RH for two to six months and 50-70% RH for two weeks demonstrated only a 2-8% decrease in reflectance for the same wavelength, even though they were also stored at elevated temperatures to accelerate the degradation process.[10] Witness samples stored in protected lab conditions show no significant degradation at $\lambda = 1050$ Å, suggesting that standard procedures such as N_2 purging when not in use and lab conditions of $\sim$ 30% RH should limit protected eLiF degradation to acceptable levels on future missions.

SPRITE's flight grating, shown in Figure 6, is the first diffraction grating to be coated with eLiF. The grating witness sample measurement in Figure 5 suggests that the eLiF coatings have improved the reflectance of the grating from the $\sim$ 73% peak achievable by conventional Lif+Al coatings to a peak reflectance of $\sim$ 82%. The grating's precise performance in the SPRITE bandpass will soon be determined.

3.2 MCP Detector

SPRITE serves as a low-Earth orbit testbed for advanced borosilicate glass MCP detectors of the type baselined in the LUVOIR and HabEx concept studies.[11] The SPRITE detector is projected to be far more resistant to the "gain sag" seen on the HST-COS MCP, which will be tested on-orbit through continuous exposure to geocoronal

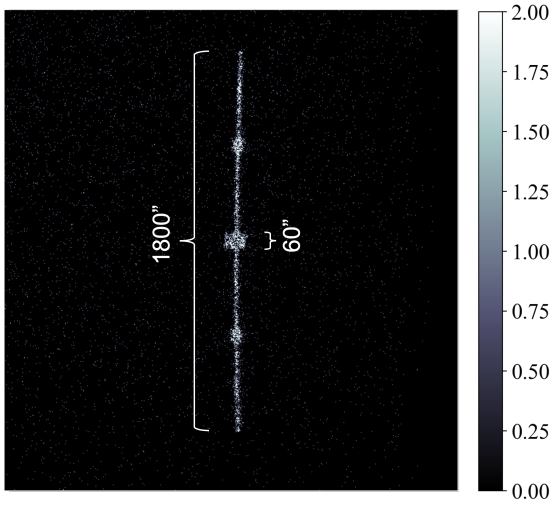

Figure 7: The SPRITE slit illuminated on the detector by overfilling with diffuse light from a Hg pen ray.

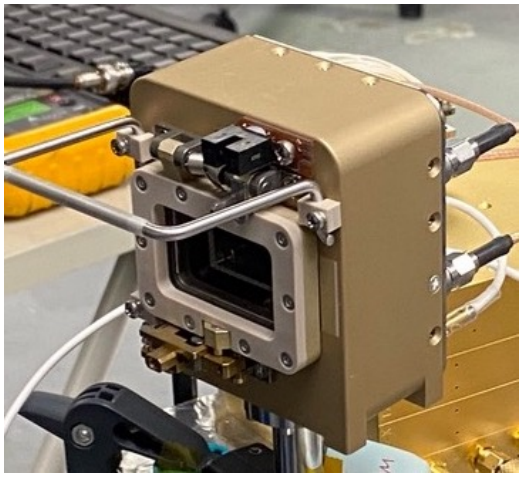

Figure 8: The MCP detector housing, shown here with its door closed, is hermetically sealed until the door is opened with a LASP-provided deployment mechanism.

Lyman alpha along the entire SPRITE slit. The spectra observed by SPRITE will be imaged on a flat 39 × 19 mm borosilicate glass MCP detector activated by ALD with a CsI photocathode with $\sim 50\mu$m resolution.[12] The SPRITE slit is imaged filled by 1849Å light from a Hg pen ray in Figure 7, with the three "point source" bulges in the slit shown. The top and bottom bulges are $30'' \times 30''$ and the central bulge is $60'' \times 60''$. These bulges provide regions of the slit for point sources in SPRITE's LyC escape survey that will reduce vignetting and have added margin for pointing instabilities.

The detector is located within a hermetically sealed housing, shown in Figure 8, evacuated to $\sim 10^{-7}$ torr at all times when in the lab. Prior to launch, the housing will be filled with UHP N_2 to 1 PSI above atmospheric pressure. A poppet relief valve will vent this gas to 1 PSI on ascent. A one-time open door on the front of the housing will deploy on-flight for an uninterrupted light path from the tertiary mirror to the face of the detector.[13] The MCP detector and its housing are provided by Sensor Sciences and are based on the JUNO-UVS detector design.[14]

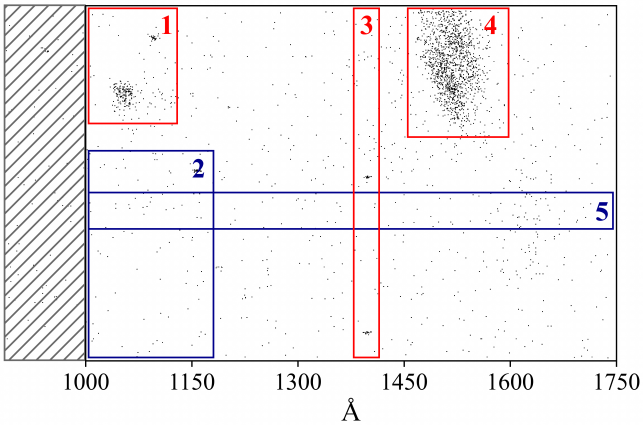

Figure 9: Sample detector background exposure. Regions 1, 3, and 4 encompass areas where there is localized field emission or where "hot spots" appear. Regions 2 and 5 highlight observational areas of interest.

Region	Count rate ($cm^{-2}\ s^{-1}$)
1	0.464
2	0.133
3	0.181
4	3.243
5	0.158
Overall	0.310
Active area*	**0.138**

Table 1: *The active area count rate excludes the areas with localized field emission areas (Regions 1, 3, and 4).

An MCP detector has several advantages, such as room temperature operation in-lab and no need for a cooling system in the CubeSat on-orbit; the most important for SPRITE's science is its exceptional noise performance. SPRITE's detector background requirement is less than 0.5 counts cm^{-2} s^{-1}, or approximately 1 count per resolution element per day. We measured the background performance of the detector in the lab with the room lights on, which likely enhances the background, by taking a set of three 1000-second "dark" exposures. We then calculated the average rate of background counts per square centimeter per second in multiple regions of the detector active area. Figure 9 shows the raw readout of one of these exposures with the five regions of interest outlined.

The active area of the detector is 39 × 19 mm; the shaded area in Figure 9 represents the leftmost 5 mm of the active area which are not illuminated by SPRITE's spectrograph. Regions 1, 3, and 4 were selected to encompass local field emission regions believed to be caused by interactions with the housing, as well as a few hot spots. Region 2 covers the wavelength range of the Lyman UV. Region 5 represents where the center of the slit falls on the active area. Table 1 shows the rate of photon counts per square centimeter per second for each region defined; the overall count rate when it is skewed by the local field emission; and the count rate of all other regions, which meets the detector background requirements with margin.

3.3 Preliminary Optical Testing

Preliminary optical alignment and testing were performed in the class 10,000 clean room at LASP. Preliminary optical illumination was done using a D_2 lamp for a continuum source, and a Hg pen-ray for a bright emission line at 1849 Å and for stray light testing.[15] A custom light source mount was designed to hold both UV light sources simultaneously, or an optical fiber-fed LED lamp for visible light tests and alignment. The lamps illuminated an F/8 parabola, providing a collimated light source for rapid testing at atmospheric pressure. To pass the UV light through the system, the entire collimator was contained in a polycarbonate box and purged with ultra-high purity (UHP) N_2 until the internal humidity was less than 5% (see Szewczyk et al., in this Proceedings).[15] This system was used to verify the focus of the EM telescope rapidly and in low humidity environments in the lab.

The EM grating was installed on the metering tower (shown in Figure 3) and aligned using a set of three adjustment screws. The grating mount and interfacing component utilize three set screws and three adjustment screws to tip/tilt/piston the grating for focusing and aligning the spectrograph. With the grating installed

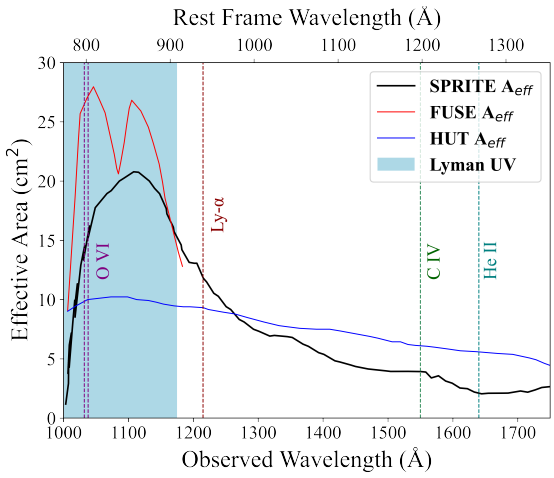

Figure 10: The projected effective area of SPRITE's instrument compared to those of FUSE and HUT based on the reflectances in Figure 5.

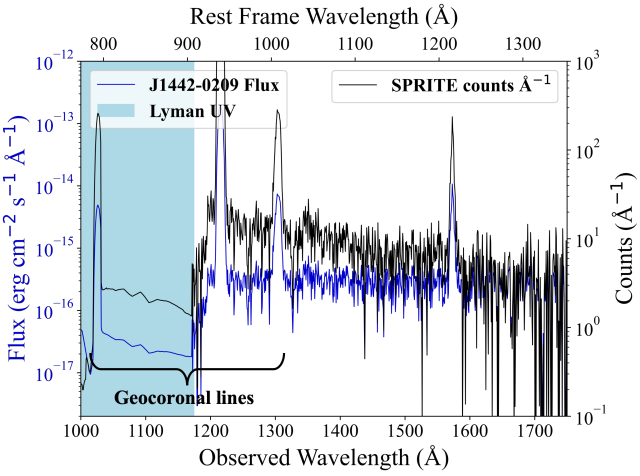

Figure 11: SPRITE's projected counts for an 80,000s exposure of J1442-0209 based on the effective area shown in Figure 10, the flux estimate in the Lyman UV by McCandliss and O'Meara (2017),[16] and the flux observed by Izotov et al. (2016)[17]

and aligned, we performed our first light test with the complete EM telescope, grating, and detector. The EM telescope's first light was from a Hg pen ray installed in the light source mount behind a 25-micron pinhole.

Data was obtained with a 2x bin factor on the detector (2048 x 2048 digital area, with ∼1375 x 775 active pixels). Using the adjustment screws on the interfacing component, the grating was aligned to place 1849Å light onto the detector, as Hg emits strongly at 1849Å. However, 1849Å was not visible as the humidity in the test setup was too high (∼ 30% RH), strongly absorbing light at $\lambda \lesssim 1900$ Å. Instead, the brightest emission feature in Figure 7 is 1942 Å, with a pseudocontinuum extending towards 1849 Å. Subsequent testing at lower humidity under purge (3-5% RH) showed the strong 1849Å feature. The SPRITE grating was canted to put these wavelengths on the detector, as they nominally are not.

The point spread function (PSF) of the focused spot corresponds to a 4Å FWHM resolution, with the cross-dispersion height at ∼100 microns, or 14″. The flight objective is < 2 Å resolution and $< 10''$ angular resolution at the slit center; however, the requirement is only 4 Å resolution to separate the O VI doublet, and $< 20''$ angular resolution. The SPRITE EM telescope therefore already meets this requirement, with further improvement expected with the flight telescope, which was measured to have half the wavefront error of the EM unit.

SPRITE's projected effective area is determined by its geometric collecting area; the reflectances of each of its optics, as shown in Figure 5; the absolute grating efficiency; and the quantum efficiency of the MCP detector. This projected effective area curve is shown in Figure 10, with notable emission lines for SPRITE's science cases labeled. SPRITE's peak effective area is ~ 21 cm^2, 75% the effective area of FUSE, despite SPRITE having less than 30% of the FUSE collecting area.

Using SPRITE's projected effective area and the MCP detector background described in Section 3.2, we can model SPRITE's projected performance for a potential Lyman UV survey target. Figure 11 shows a spectrum of J1442-0209 as projected through the SPRITE effective area. J1442-0209 is a known LyC emitter from Izotov et al. (2016) as observed by HST-COS. SPRITE readily detects the LyC detected by COS, as well as nearly 100 additional angstroms due to the larger bandpass of SPRITE.

4. FURTHER INTEGRATION AND TESTING

The next phase of testing for the EM telescope will occur in the CUSP/LASP Long Tank calibration facility, a 30-foot-long clean vacuum chamber.[18] This chamber is designed to point collimated light down the length of the tank. SPRITE will be installed on a tip-tilt mount at the end of the chamber to allow for fine adjustment to align the telescope with the collimated beam. Further GSE development required for the safety of the MCP detector while it is in the Long Tank is described in Szewczyk et al. (2023). Testing in the Long Tank chamber will provide a flightlike environment in which we can take and analyze test data in real time.

Finally, all characterization testing on the EM telescope must be repeated on the flight telescope so that its performance can be quantified prior to environmental and non-instrument integration and testing. As this is the first time the test setups described in this paper and in Szewczyk et al. (2023) have been used, the project is continuing to qualify the test setups, particularly with vacuum testing in the Long Tank pending. Given the environmental sensitivity of the optics, the flight instrument will not be used until all tests are completed and validated. This testing validation model was used during the CUTE program.[19]

The extended I&T campaign will include electronics integration and environmental testing, including thermal vacuum (TVAC) testing and vibrational testing. After environmental testing, we will perform comprehensive hardware inspections and instrument performance tests.

5. CONCLUSIONS

The SPRITE instrument features a unique design with similarly unique challenges for integration and testing. The preliminary optical testing and characterization of the SPRITE EM telescope yielded results that met or exceeded all mission requirements. The preliminary successes of the enhanced LiF+Al coatings demonstrate that SPRITE will achieve highly sensitive measurements in-flight and qualify these coatings for use on future NASA missions. Through these advanced optical coatings and an extensive test program with significant student

involvement, SPRITE is projected to achieve Explorer-class sensitivities with a CubeSat budget. The project anticipates the remainder of our I&T phase to continue until mid-2024.

The advanced optical coatings and photon-counting MCP detector utilized for SPRITE represent a new generation of FUV astrophysical surveys.[20] SPRITE will address a significant and scientifically rich gap in spectral observations of energetic galactic regions. In doing so, SPRITE will demonstrate that low-cost CubeSat missions can perform operationally challenging FUV observations and provide high-impact results for astrophysics science objectives.

ACKNOWLEDGMENTS

This work was funded by a grant from NASA, Award no. 80NSSC19K0995, to the University of Colorado. The authors extend many thanks to all of the staff and students at CUSP and LASP who have contributed their time and effort to the project.

REFERENCES

[1] Fleming, B., France, K., Williams, J., Ulrich, S., Tumlinson, J., McCandliss, S., O'Meara, J., Sankrit, R., Borthakur, S., Jaskot, A., Rutkowski, M., Quijada, M., Hennessy, J., and Siegmund, O., "High-sensitivity far-ultraviolet imaging spectroscopy with the SPRITE Cubesat," in [*UV, X-Ray, and Gamma-Ray Space Instrumentation for Astronomy XXI*], Siegmund, O. H., ed., **11118**, 236 – 247, International Society for Optics and Photonics, SPIE (2019).

[2] National Academies of Sciences, E. and Medicine, [*Pathways to Discovery in Astronomy and Astrophysics for the 2020s*], The National Academies Press, Washington, DC (2021).

[3] Indahl, B., Fleming, B., Vorobiev, D., Chafetz, D., Williams, J., Bowen, M., Brening, D., Borthakur, S., Del Hoyo, J., DeWitt, D., Diaz, A., Durell, A., Foehr, B., France, K., Gopinathan, S., Hennessy, J., Jaskot, A., Kaiser, M., Koehler, S., Magruder, A., McCandliss, S., O'Meara, J., Quijada, M., Rodríguez-de Marcos, L., Rutkowski, M., Sankrit, R., Sico, A., Siegmund, O., Szewczyk, D., Tumlinson, J., and Ulrich, S., "Status and mission operations of the SPRITE 12U CubeSat: a probe of star formation feedback from stellar to galactic scales with far-UV imaging spectroscopy," in [*Society of Photo-Optical Instrumentation Engineers (SPIE) Conference Series*], *Society of Photo-Optical Instrumentation Engineers (SPIE) Conference Series* **12678** (Aug. 2023).

[4] Green, J. C., Froning, C. S., Osterman, S., Ebbets, D., Heap, S. H., Leitherer, C., Linsky, J. L., Savage, B. D., Sembach, K., Shull, J. M., Siegmund, O. H. W., Snow, T. P., Spencer, J., Stern, S. A., Stocke, J., Welsh, B., Béland, S., Burgh, E. B., Danforth, C., France, K., Keeney, B., McPhate, J., Penton, S. V., Andrews, J., Brownsberger, K., Morse, J., and Wilkinson, E., "The Cosmic Origins Spectrograph," **744**, 60 (Jan. 2012).

[5] Fleming, B., Quijada, M., Hennessy, J., Egan, A., Hoyo, J. D., Hicks, B. A., Wiley, J., Kruczek, N., Erickson, N., and France, K., "Advanced environmentally resistant lithium fluoride mirror coatings for the next generation of broadband space observatories," *Appl. Opt.* **56**, 9941–9950 (Dec 2017).

[6] Ohl, R. G., Barkhouser, R. H., Conard, S. J., Friedman, S. D., Hampton, J., Moos, H. W., Nikulla, P., Oliveira, C. M., and Saha, T. T., "Performance of the Far Ultraviolet Spectroscopic Explorer mirror assemblies," in [*Instrumentation for UV/EUV Astronomy and Solar Missions*], Fineschi, S., Korendyke, C. M., Siegmund, O. H. W., and Woodgate, B. E., eds., **4139**, 137 – 148, International Society for Optics and Photonics, SPIE (2000).

[7] Team, T. L., "The luvoir mission concept study final report," (2019).

[8] Hennessy, J., Jewell, A., Jones, J.-P., Crouch, G., and Nikzad, S., "Aluminum precursor interactions with alkali compounds in thermal atomic layer etching and deposition processes," *ACS Applied Materials Interfaces* **13** (01 2021).

[9] Oliveira, C. M., Retherford, K., Conard, S. J., Barkhouser, R. H., and Friedman, S. D., "Aging studies of LiF-coated optics for use in the far ultraviolet," in [*EUV, X-Ray, and Gamma-Ray Instrumentation for Astronomy X*], Siegmund, O. H. W. and Flanagan, K. A., eds., **3765**, 52 – 60, International Society for Optics and Photonics, SPIE (1999).

[10] Rodríguez-de Marcos, L., Fleming, B., Hennessy, J., Chafetz, D., Del Hoyo, J., Quijada, M., Bowen, M., Vorobiev, D., and Indahl, B., "Advanced Al/eLiF mirrors for the SPRITE CubeSat," in [*Society of Photo-Optical Instrumentation Engineers (SPIE) Conference Series*], *Society of Photo-Optical Instrumentation Engineers (SPIE) Conference Series* **12188**, 1218820 (Aug. 2022).

[11] Siegmund, O. H. W., Ertley, C., Vallerga, J. V., Schindhelm, E. R., Harwit, A., Fleming, B. T., France, K. C., Green, J. C., McCandliss, S. R., and Harris, W. M., "Microchannel plate detector technology potential for LUVOIR and HabEx," in [*UV, X-Ray, and Gamma-Ray Space Instrumentation for Astronomy XX*], Siegmund, O. H., ed., **10397**, 282 – 295, International Society for Optics and Photonics, SPIE (2017).

[12] Siegmund, O. H. W., Richner, N., Gunjala, G., McPhate, J. B., Tremsin, A. S., Frisch, H. J., Elam, J., Mane, A., Wagner, R., Craven, C. A., and Minot, M. J., "Performance characteristics of atomic layer functionalized microchannel plates," in [*UV, X-Ray, and Gamma-Ray Space Instrumentation for Astronomy XVIII*], Siegmund, O. H., ed., **8859**, 88590Y, International Society for Optics and Photonics, SPIE (2013).

[13] Chafetz, D., Fleming, B. T., Williams, J., Fotherby, R. L., Tompkins, A., Anderson, N. K., Kohnert, R., France, K., Vorobiev, D., and Siegmund, O., "Mechanical design and development of SPRITE: a 12U CubeSat with a far-ultraviolet imaging spectrograph," in [*UV, X-Ray, and Gamma-Ray Space Instrumentation for Astronomy XXII*], Siegmund, O. H., ed., **11821**, 134 – 148, International Society for Optics and Photonics, SPIE (2021).

[14] Gladstone, G. R., Persyn, S. C., Eterno, J. S., Walther, B. C., Slater, D. C., Davis, M. W., Versteeg, M. H., Persson, K. B., Young, M. K., Dirks, G. J., Sawka, A. O., Tumlinson, J., Sykes, H., Beshears, J., Rhoad, C. L., Cravens, J. P., Winters, G. S., Klar, R. A., Lockhart, W., Piepgrass, B. M., Greathouse, T. K., Trantham, B. J., Wilcox, P. M., Jackson, M. W., Siegmund, O. H. W., Vallerga, J. V., Raffanti, R., Martin, A., Gérard, J. C., Grodent, D. C., Bonfond, B., Marquet, B., and Denis, F., "The Ultraviolet Spectrograph on NASA's Juno Mission," **213**, 447–473 (Nov. 2017).

[15] Szewczyk, D., Bowen, M., Indahl, B., Vorobiev, D., Durell, A., Rodríguez-de Marcos, L., Hennessy, J., and Fleming, B., "Advanced Al/eLiF mirrors for the SPRITE CubeSat," in [*Society of Photo-Optical Instrumentation Engineers (SPIE) Conference Series*], *Society of Photo-Optical Instrumentation Engineers (SPIE) Conference Series* **12678** (Aug. 2023).

[16] McCandliss, S. R. and O'Meara, J. M., "Flux sensitivity requirements for the detection of lyman continuum radiation drop-ins from star-forming galaxies below redshifts of 3," *The Astrophysical Journal* **845**, 111 (aug 2017).

[17] Izotov, Y. I., Schaerer, D., Thuan, T. X., Worseck, G., Guseva, N. G., Orlitová , I., and Verhamme, A., "Detection of high lyman continuum leakage from four low-redshift compact star-forming galaxies," *Monthly Notices of the Royal Astronomical Society* **461**, 3683–3701 (may 2016).

[18] France, K., Hoadley, K., Fleming, B. T., Kane, R., Nell, N., Beasley, M., and Green, J. C., "The SLICE, CHESS, and SISTINE Ultraviolet Spectrographs: Rocket-Borne Instrumentation Supporting Future Astrophysics Missions," *Journal of Astronomical Instrumentation* **5**, 1640001 (Dec. 2016).

[19] Egan, A., France, K., Nell, N., DeCicco, N., Suresh, A., Kohnert, T., Fleming, B., and Ulrich, S., "The Colorado Ultraviolet Transit Experiment: Integration, Testing, and Lessons Learned on a NASA Astrophysics CubeSat," in [*Small Satellite Conference 2022*], *Small Satellite Conference Series* (2022).

[20] Quijada, M. A., Hoyo, J. D., and Rice, S., "Enhanced far-ultraviolet reflectance of MgF2 and LiF overcoated Al mirrors," in [*Space Telescopes and Instrumentation 2014: Ultraviolet to Gamma Ray*], Takahashi, T., den Herder, J.-W. A., and Bautz, M., eds., **9144**, 1357 – 1366, International Society for Optics and Photonics, SPIE (2014).